Variational Continuous Assimilation of TMI and SSM/I Rain Rates: Impact on GEOS-3 Hurricane Analyses and Forecasts

ARTHUR Y. HOU, SARA Q. ZHANG,* AND ORESTE REALE+

Global Modeling and Assimilation Office, NASA Goddard Space Flight Center, Greenbelt, Maryland

(Manuscript received 27 June 2003, in final form 6 January 2004)

ABSTRACT

This study describes a 1D variational continuous assimilation (VCA) algorithm for assimilating tropical rainfall data using moisture/temperature time-tendency corrections as the control variable to offset model deficiencies. For rainfall assimilation, model errors are of special concern since model-predicted precipitation is based on parameterized moist physics, which can have substantial systematic errors. The authors examine whether a VCA scheme using the forecast model as a weak constraint offers an effective pathway to precipitation assimilation.

The particular scheme investigated employs a precipitation observation operator based on a 6-h integration of a column model of moist physics from the Goddard Earth Observing System (GEOS) global data assimilation system (DAS). In earlier studies, a simplified version of this scheme was tested, and improved monthly mean analyses and better short-range forecast skills were obtained. This paper describes the full implementation of the 1DVCA scheme using background and observation error statistics and examines its impact on GEOS analyses and forecasts of prominent tropical weather systems such as hurricanes.

Assimilation experiments with and without rainfall data for Hurricanes Bonnie and Floyd show that assimilating 6-h Tropical Rainfall Measuring Mission (TRMM) Microwave Imager (TMI) and Special Sensor Microwave Imager (SSM/I) surface rain accumulations leads to more realistic analyzed storm features and better 5-day storm track prediction and precipitation forecasts. These results demonstrate the importance of addressing model deficiencies in moisture time tendency in order to make effective use of precipitation information in data assimilation.

1. Introduction

Precipitation estimates from spaceborne passive microwave instruments such as the Tropical Rainfall Measuring Mission (TRMM) Microwave Imager (TMI) and Special Sensor Microwave Imager (SSM/I) have been assimilated using a variety of techniques to improve global atmospheric analyses and forecasts (e.g., Krishnamurti et al. 1993; Tsuyuki 1997; Hou et al. 2000a; Treadon et al. 2002; Marecal and Mahfouf 2002). Currently, operational global weather forecast systems typically use a multidimensional variational scheme to optimize the initial condition of a forecast but do not address deficiencies in the forecast model. Since rainfall in global models is based on parameterized moist physics with simplifying assumptions, which can have significant systematic errors (Randall et al. 2003), it is important to consider model errors in precipitation assimilation. There is ample evidence that analyses in the Tropics are sensitive to the treatment of diabatic processes (e.g., Trenberth and Olson 1988), suggesting that deficiencies in moist physics schemes can be an important source of analysis errors, especially in regions with sparse observations.

Since systematic model errors can lead to poor forecasts even with perfect initial conditions, the influence of model errors needs to be considered in order to assimilate precipitation information effectively in the presence of model biases. Typically, errors in physical parameterizations are projected as state-dependent systematic errors in forecast tendencies, which are difficult to quantify without dense observation networks. The challenge of developing assimilation algorithms to account for systematic model errors is very much hindered by the lack of a priori knowledge of the nature of these errors. In the coming years more microwave rainfall data will become available from operational and research satellites, culminating in a constellation of eight or more satellites to provide global rain measurements every 3 h with the proposed Global Precipitation Measurement (GPM) mission. The ability to assimilate rainfall information effectively in the presence of forecast model

* Additional affiliation: Science Applications International Corp., Beltsville, Maryland.

+ Additional affiliation: University of Maryland, Baltimore County, Baltimore, Maryland.

Corresponding author address: Dr. Arthur Y. Hou, NASA Goddard Space Flight Center, Code 900.3, Greenbelt, MD 20771.
E-mail: arthur.y.hou@nasa.gov

biases will be crucial for realizing the full benefit from these observations.

This study extends our earlier research (Hou et al. 2000a,b, 2001) to examine an alternative rainfall assimilation strategy using forecast tendency corrections as a control variable within the general framework of variational continuous assimilation (VCA; Derber 1989) to compensate for model deficiencies. Since model-predicted precipitation is diagnostically linked to the time rate of change in temperature and in moisture associated with parameterized moist physics, the VCA approach offers a natural framework for assimilating precipitation data using moisture and temperature tendencies as the control variables. We have been exploring the effectiveness of such a strategy using a 1DVCA algorithm to assimilate 6-h accumulated TMI and SSM/I tropical rainfall in the Goddard Earth Observing System (GEOS) global data assimilation system (DAS). The forward model for precipitation is based on a 6-h integration of a column model of the GEOS moist physics with prescribed large-scale forcing from the full GEOS DAS.

In previous studies (Hou et al. 2000a,b, 2001), before quantitative error estimates for microwave-based rain retrievals became available, we had examined the 1DVCA scheme with several simplifications: (i) the cost function consisted only of the observation term, (ii) the correction was applied only to the model's moisture tendency, and (iii) the moisture tendency correction had a prescribed vertical structure mimicking the Jacobian of the 6-h rain accumulation to moisture perturbations. Results showed that, even with these simplifications, assimilating TMI and SSM/I tropical rain rates together with total precipitable water (TPW) estimates using this procedure is effective in improving GEOS analyses and aspects of short-range forecasts. Notably, it improves not only 6-h averaged analyses of precipitation and moisture but also related climate parameters such as clouds and atmospheric radiation fluxes, as verified against the top-of-the-atmosphere radiation measurements from Clouds and the Earth's Radiation Energy System (CERES) sensors and brightness temperatures for moisture-sensitive channels of the High Resolution Infrared Radiation Sounder (HIRS).

This paper describes the full implementation of the 1DVCA scheme using background and observation error information together with an extended control variable that includes both moisture and temperature time-tendency corrections without imposed vertical structures as done in Hou et al. (2001). In our previous work, we assessed the impact of precipitation assimilation on the monthly mean $2^\circ \times 2.5^\circ$ GEOS analyses and forecasts (Hou et al. 2001). The present investigation focuses on the impact of assimilating 6-h tropical TMI and SSM/I rain accumulation on $1^\circ \times 1^\circ$ GEOS version 3 (GEOS-3) synoptic analyses and forecasts of two hurricanes, Bonnie (1998) and Floyd (1999). Section 2 outlines the general methodology. Section 3 discusses implementation details and data usage in the GEOS-3 DAS. Section 4 describes the Bonnie and Floyd assimilation experiments. Sections 5 and 6 evaluate the impact of precipitation assimilation on GEOS-3 analyses and forecasts, respectively. Section 7 summarizes the main results.

2. Methodology

Variational algorithms for precipitation assimilation typically seek to minimize a functional that measures the misfit between the model-predicted rain and the observed rain with respect to a control variable to which the model rain is sensitive. The control variable may be the initial condition (as in a conventional 4D variational scheme), a model attribute (such as the forecast time tendency in a VCA scheme), or some combination of both (e.g., Zupanski et al. 2002). Since analysis techniques are built upon the assumption that the underlying error statistics are random, unbiased, stationary, and normally distributed, it is crucial that biases in the forecast model be removed (Dee and Todling 2000). However, in the case of precipitation, errors in the model-predicted rain derived from parameterized physics are invariably systematic and state dependent. In this section we describe a 1DVCA procedure to assimilate observed surface rain rates to estimate and correct for systematic errors in time tendencies of temperature and/or moisture within a 6-h assimilation cycle. The functional to be minimized is

$$J(\delta\mathbf{w}) = (\delta\mathbf{w})^{\mathrm{T}}\mathbf{Q}^{-1}(\delta\mathbf{w}) + (y - y^o)^{\mathrm{T}}\mathbf{R}^{-1}(y - y^o), \quad (1)$$

where $y = \log[H(\delta\mathbf{w})]$, with H being the precipitation observation operator, and y^o the logarithm of the observed rain, with the logarithmic singularity removed with a minimal threshold value of 0.01 mm day^{-1}; $\mathbf{R}$ is the ''observation'' error covariance, which includes nonsystematic errors in both observations and the forward model. Since precipitation is a nonnegative quantity, a logarithmic transformation is used so that the observation error in terms of the relative error defined as $\varepsilon^o = y^o/y^t$ (where y^t is the true rain rate) has an approximately lognormal distribution. With this transformation, for an unbiased observation, $\langle\varepsilon^o\rangle = 1$, and $R_{ij} = \log\langle\varepsilon_i^o\varepsilon_j^o\rangle$, where i and j are row and column indices (Cohn 1997). The control variable, $\delta\mathbf{w} = (\delta q/q_s^b, \delta T)^{\mathrm{T}}$, which is held constant within a 6-h window, consists of a temperature time-tendency correction, δT, and a moisture time-tendency correction on the pseudo–relative humidity, $\delta q/q_s^b$, where q_s^b is the background saturation specific humidity, and the background can be a forecast or a preanalysis (see section 3). The transformation from specific humidity to pseudo–relative humidity is consistent with the treatment of moisture in the GEOS-3 analysis to obtain better background error covariance models (Dee and da Silva 2003). The vector dimension of $\delta\mathbf{w}$ is $2N$, where N is the number of vertical model levels; $\mathbf{Q}$ is the error covariance for a prior estimate of $\delta\mathbf{w}$.

For assimilating 6-h rain accumulation averaged over a model grid, the model rain is obtained from a 6-h integration of a nonlinear column model of GEOS-3 moist physics, M, as a function of the state vector of temperature and specific humidity, $\mathbf{x} = (T, q)$:

$$\partial\mathbf{x} = M\mathbf{x} + F + \delta\mathbf{x}, \tag{2}$$

where ∂_t denotes the partial derivative with respect to time, and F is the net time tendency due to processes other than moist physics prescribed from a 3-h assimilation by the full GEOS-3 DAS from the beginning of the analysis cycle (see Hou et al. 2000a for details). Included in F are contributions from dynamics, turbulence, radiation, and incremental analysis update (IAU) forcing due to all observations except precipitation. Since moist convection schemes used in global models are parameterized to represent ensemble averages of cloud and precipitation over a convective life cycle, some temporal and spatial averaging of the instantaneous observations at satellite footprint scales is necessary in constructing the precipitation forward model for physical consistency. The observation operator for 6-h surface rain accumulation, H, may be written as

$$H(\delta\mathbf{w}) = -\int_0^{\Delta\tau}\int_0^h \rho\partial_t q(\delta\mathbf{w})\, dz\, dt, \quad \text{for } \partial_t q < 0, \tag{3}$$

where $\partial_t q$ is the moisture time tendency in specific humidity, $\Delta\tau$ is the width of the analysis window, and h is the model top.

Consistent with the use of a column model for precipitation, rain rates are assumed to be uncorrelated horizontally, in which case $\mathbf{R}$ reduces to a scalar, R, given by the variance of *relative* observation errors in retrieved rain rates (assuming negligible random errors in the forward model), namely, $R = \log[1 + (\sigma^o)^2]$, where σ^o is the error standard deviation given by $\langle(\varepsilon^o - 1)^2\rangle^{1/2}$ for rain rates greater than 0.1 mm h^{-1}. Bauer et al. (2002) estimated that the error standard deviation of instantaneous TMI retrievals averaged to 60-km grids ranges from 20%–50% at low rain rates (e.g., 0.1 mm h^{-1}) to 5%–20% at high rain rates (e.g., 20 mm h^{-1}). For 100-km averages, the errors are estimated to be less than 30% at low rain rates and 10% at high rain rates. Taking into account of additional errors arising from undersampling by TRMM overpasses in a 6-h interval on the order of 20%–60% (Bell et al. 1990), σ^o is assumed to be 15%–50% for 6-h TMI rain averaged to 1° latitude by 1° longitude grids. In this study σ^o is taken to be 0.3 for rain rates greater than 0.1 mm h^{-1}, below which σ^o is set to 0.7, reflecting greater uncertainties in relative errors at very low rain rates. These values are by no means definitive but provide a reasonable starting point. These same σ^o values are also used for SSM/I rain rates, even though TMI retrievals are expected to be of higher quality due to its lower orbit. But the differences between TMI and SSM/I retrievals are likely smaller than uncertainties in the intrinsic errors in each (W. Olson 2002, personal communication).

The specification of the 1D model error covariance matrix, $\mathbf{Q}$, requires a quantitative knowledge of errors in temperature and moisture tendencies of the forecast model beyond our current understanding. Until better information becomes available, a starting point for modeling $\mathbf{Q}$ is to parameterize it in terms of the background temperature and moisture errors based on the statistics of observation-minus-forecast (O–F) residuals. As discussed in Dee and da Silva (2003), transforming the moisture variable from specific humidity to pseudo–relative humidity has the advantage of rendering $\mathbf{Q}$ more homogeneous in space and time, and therefore more consistent with the underlying statistical assumptions of the analysis method.

The solution to (1) is obtained by minimizing $J(\delta\mathbf{w})$ with respect to $\delta\mathbf{w}$ using a quasi-Newton method. For a nonlinear observation operation, the gradient of J given by

$$\nabla J = \mathbf{Q}^{-1}\delta\mathbf{w} + [\partial y/\partial(\delta\mathbf{w})]\mathbf{R}^{-1}(y - y^o), \tag{4}$$

which must be computed at each iteration, with the vertical structure of $\delta\mathbf{w}$ given by $\mathbf{Q}$ and the updated Jacobian of H. An advantage of the limited dimension of a column model is that ∇J may be computed numerically using a standard perturbation method.

Compared with other techniques, the 1DVCA scheme differs from nudging or physical initialization in that it is a statistical analysis within the optimal estimation framework, even though they all explicitly modify the prognostic equations. As implemented in the GEOS DAS, the VCA scheme effectively operates as an online model bias estimation and correction for precipitation and moisture every 6 h, similar in principle to the bias correction procedure described in Dee and Todling (2000). The main differences are that in our case the bias estimation and correction are carried out throughout the model integration and that, unlike the moisture analysis per se, there is no a priori assumption that systematic errors in moisture tendencies associated with precipitation processes are slowly varying. By assimilating 6-h rain accumulation with online bias corrections, the VCA scheme has the advantage of virtually eliminating situations with zero background rain, which is an issue in assimilating instantaneous rain rates within a static one-dimensional variational data assimilation/three-dimensional variational data assimilation (1DVAR/3DVAR) framework since the observation operator is inactive (Fillion and Errico 1997; Treadon et al. 2002). In its generalization to four dimensions, the VCA scheme is similar to four-dimensional variational data assimilation (4DVAR) schemes that employ the forecast model as a weak constraint. However, as a technique for precipitation analysis, the VCA scheme differs from other schemes in that the VCA-based precipitation estimate is not a forecast product but is determined by the

TABLE 1. GEOS-3 background error standard deviations for q/q_s^b and T used to prescribe the error standard deviations for $\Delta\mathbf{w} = (\Delta q/q_s^b, \Delta T)$. For reference, the values of pseudo–relative humidity are converted to specific humidity using a typical saturation specific humidity profile for the Tropics.

Pressure (h Pa)	q/q_s^b	q (g kg^{-1})	T (K)
327	0.18	0.25	0.40
392	0.20	0.50	0.40
462	0.20	1.00	0.42
535	0.19	1.10	0.34
609	0.19	1.70	0.30
680	0.19	1.90	0.32
748	0.17	2.40	0.40
808	0.16	2.40	0.54
858	0.15	2.40	0.68
899	0.13	2.40	0.82
930	0.11	2.20	0.86
954	0.10	2.10	0.90
971	0.09	2.00	0.94
983	0.08	1.90	0.96
991	0.08	1.90	0.96
995	0.08	1.90	1.00

6-h rain accumulation from a continuous 4D data assimilation constrained by precipitation observations.

3. Implementation and data usage in GEOS-3 DAS

The 1DVCA procedure may be implemented as an online bias estimation/correction scheme to improve the first guess in an intermittent data assimilation system. But, in the GEOS-3 DAS, which uses an IAU scheme to distribute the influence of analysis increments as a constant forcing over the analysis time window (Bloom et al. 1996), it is natural to use the VCA scheme to estimate model time-tendency corrections based on precipitation data to be added to the IAU forcing due to other data types. This is accomplished by performing the 1DVCA precipitation assimilation after a preanalysis within a 6-h assimilation cycle using the standard Physical-space Statistical Analysis System (PSAS; Cohn et al. 1998), which consists of a multivariate analysis of wind, height, and surface pressure and a univariate analysis of moisture using conventional observations, SSM/I surface wind speed and TPW data, and online temperature and moisture retrievals from Television Infrared Observation Satellite (TIROS) Operational Vertical Sounder (TOVS). This preanalysis provides the large-scale forcing and IAU tendencies for the column model (2) and the background rain for quality control decisions. The final GEOS-3 assimilation consists of a time integration of the forecast model under incremental IAU tendency forcing over 6 h to provide instantaneous analyses of prognostic variables and 6-h averaged diagnostic quantities (e.g., precipitation) at analysis times (0000, 0600, 1200, 1800 UTC).

A distinctive feature of the GEOS-3 DAS is that the IAU scheme virtually eliminates the need for an explicit initialization and any spinup in the precipitation and evaporation fields (Schubert et al. 1993). The GEOS-3 DAS is an upgraded GEOS system that uses an interactive mosaic-type land surface model and online temperature and moisture retrievals using TOVS radiances. The model rain consists of convective precipitation generated by the relaxed Arakawa–Schubert (RAS) scheme (Moorthi and Suarez 1992) with a Kessler-type reevaporation of falling rain and large-scale precipitation from supersaturation (Kessler 1969).

In the GEOS-3 DAS, precipitation assimilation is implemented subject to the constraint that the column moisture does not depart by more than a few percent from the preanalyzed TPW, which includes contributions from SSM/ITPW data. This is accomplished by solving (1) with the additional term $(\sigma^{\mathrm{TPW}})^{-2}(\delta Z)^2$, where,

$$\delta Z = \int_0^{\Delta\tau} \int_0^h \delta q(z)\, dz\, dt, \tag{5}$$

and σ^{TPW} is assigned a small value of 0.05 to effectively preserve the preanalyzed TPW value. The quasi-Newton minimization algorithm typically converges between 5 and 25 iterations.

a. Sensitivity to temperature and moisture time-tendency adjustments

In the general formulation of the VCA scheme, time-tendency corrections of temperature and moisture, the two inputs for updating the moist physics at each time step, may be used as the control variable in minimizing (1). In earlier studies (Hou et al. 2000a,b, 2001), only δq was used. Here we investigate whether a better model-observation fit in 6-h rain can be obtained by including δT in the control variable. But, as discussed in section 2, there is as yet insufficient knowledge to fully specify the model error covariance matrix. In this study, $\mathbf{Q}$ is simplified to consist of only diagonal elements given by the error variances of the background state. Specifically, Δq and ΔT (i.e., the total δq and δT summed over 6 h, respectively) are assumed to have the same error standard deviations as q and T in the GEOS-3 DAS, as given in Table 1. Note that for this diagonal $\mathbf{Q}$ matrix, the Hessian is positive definite, which guarantees convergence.

We performed three offline tests to examine the sensitivity of the minimization solution to temperature and moisture tendency adjustments within the limitations of the simplified $\mathbf{Q}$. The experiments compared three different configurations of the control variables: one with δq and δT, one with only δq, and one with only δT. Table 2 shows that, in terms of the misfit in 6-h rain between the model and observations, using both δq and δT as the control variable gives virtually the same result as using only δq, whereas using δT alone is much less effective in minimizing the misfit. Thus, the 6-h rain

TABLE 2. Rms errors in 6-h rain rate at a sample analysis time.

Control variable	No. of cases	O–B (mm h^{-1})	O–A (mm h^{-1})		
			$\delta q + \delta T$	δq	δT
O–B $<$ 0 cases	310	0.92	0.46	0.44	0.68
O–B $>$ 0 cases	140	1.33	0.78	0.74	1.22

accumulation is more sensitive to incremental δq adjustments than δT adjustments. This relative insensitivity to small incremental δT adjustments over 6 h is in contrast to the behavior of precipitation over one physics time step (10 min), which can be more responsive to initial temperature adjustments within one error standard deviation of the background temperature.

However, unlike the 6-h rain, the solution for $\delta\mathbf{w}$, whose vertical structure depends upon both $\mathbf{Q}$ and the sensitivity of H to time-continuous temperature and moisture tendency perturbations, is affected by the presence of δT. The RAS type of convective scheme has previously been shown to be responsive to both moisture and temperature perturbations (Fillion and Errico 1997; Fillion and Mahfouf 2000). Figure 1 shows the Jacobian of H for 6-h total (convective and large scale) rain to *persistent* perturbations in moisture and temperature *time tendencies* at two locations: one consisting of only convective rain from RAS and the other with mostly large-scale rain from supersaturation. The perturbation amplitude at each time step is 5×10^{-9} g kg^{-1} s^{-1} for δq and 5×10^{-9} K s^{-1} for δT. Both perturbations are applied up to 300 hPa, the highest level of moisture analysis. The sensitivity to δq perturbations peaks at the cloud base near the surface for convective precipitation, in contrast to a more uniform response in height with a maximum aloft in the case of the large-scale rain. The rain Jacobian to δT perturbations also shows significant responses at all levels for both convective and large-scale processes.

In Fig. 2, solutions for the ensemble-mean Δq and ΔT from the three offline tests are shown separately for 310 negative observation-minus-background (O–B) cases and 140 O–B $>$ 0 cases, collected over tropical locations in one 6-h analysis window. The background rain is obtained from (3) with $\delta\mathbf{w} = 0$. The solution for Δq (with or without ΔT in the control variable) shows a concentrated low-level maximum, similar to the Jacobian for 6-h convective precipitation in Fig. 1, suggesting that the tendency corrections are dominated by convective rain events. The ad hoc assumption that Δq decreases with height used in earlier investigations (e.g., Hou et al. 2001) is therefore a reasonable approximation for the GEOS system, though clearly inappropriate for locations where the large-scale rain dominates. In the present study the rain Jacobian is explicitly computed in solving (1), which eliminates this pitfall. The inclusion of ΔT reduces the burden on Δq in minimizing (1), leading to a smaller low-level maximum and a broadening of the vertical profile in Δq, as seen in Fig. 2. However, unlike Δq, which is considerably larger than the model error standard deviations at the low levels, ΔT adjustments are small at all heights relative to the prescribed error standard deviations given in Table 1. Figure 2 also shows that the actual Δq values used in online assimilation experiments are significantly smaller than the offline solutions as a result of the added TPW constraint in the cost function and quality control. Moreover, the net changes in moisture over 6 h in online experiments tend to be less than Δq because of feedbacks from the model physics (see Hou et al. 2000a, section 3e). However, online Δq values can lead to 6-h changes in q greater than two standard deviations of the background moisture, which are rejected by the after-analysis quality control (QC) check (see section 3b and Table 3).

The above results show that δq is much more effective

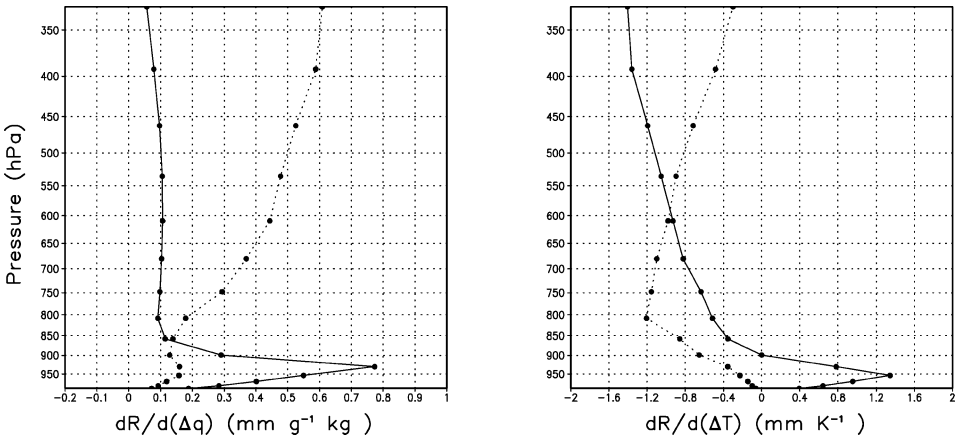

FIG. 1. Jacobians of 6-h column model rain to persistent perturbations in time tendencies of moisture and temperature; Δq and ΔT are the total perturbations in moisture and temperature tendencies summed over 6 h, respectively. The solid line is for a model grid location with only convective rain (R_c = 1.3 mm h^{-1}). The dashes are for a location dominated by large-scale rain (R_{LS} = 5.6 mm h^{-1}; R_c = 0.4 mm h^{-1}).

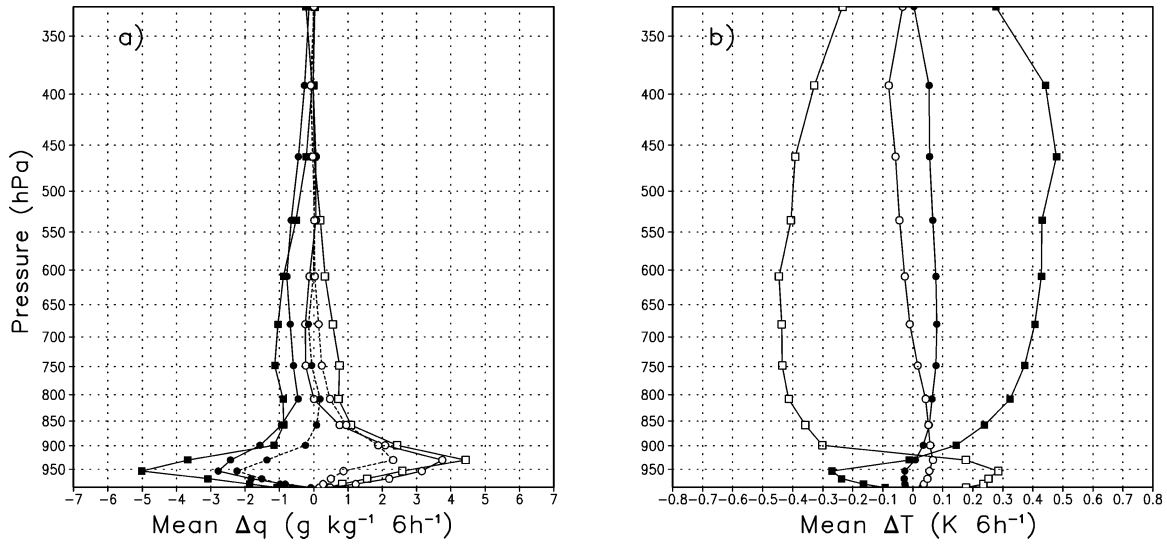

FIG. 2. Offline minimization solutions to (1) for the results shown in Table 2. (a) Solid lines are ensemble-mean Δq for 310 cases of O–B < 0 (closed symbols) and 140 cases of O–B > 0 (open symbols). The circles are solutions obtained using $\Delta q + \Delta T$ as the control variable. The squares are solutions using only Δq as the control variable. The dashes show typical Δq values from an online assimilation. (b) Corresponding ensemble-mean ΔT using $\Delta q + \Delta T$ as the control variable, with closed circles for O–B < 0 cases and open circles for O–B > 0 cases. The closed and open squares show solutions obtained using only ΔT as the control variable for O–B < 0 and O–B > 0 cases, respectively.

than δT in bringing the model rain closer to observations and thus is a key variable for assimilating 6-h precipitation using the 1DVCA algorithm. The addition of δT in the control variable does not improve the precipitation or directly alter the temperature appreciably in the analysis but can have a significant impact on δq, which would, in turn, affect how rainfall assimilation influences other analysis variables. However, the true influence of δT on δq cannot be determined without knowing the cross correlation between the two variables or considering their vertical correlations. Given the ad hoc nature of the simple **Q** matrix used in this study, results of these offline tests are suggestive of the importance of considering δT adjustments but can not capture the true influence of δT on the analysis. With this in mind, we will limit the scope of the remaining study to examining the 1D VCA rainfall assimilation scheme using only δq, which effectively reduces the dimension of the control variable by half for greater computational efficiency.

TABLE 3. Data usage at tropical TMI+SSM/I observation locations at 1200 UTC 20 Aug 1998.

Observation	Background	No. of observations*	|O–B| > 0.17 (mm h^{-1})	|O–B| < 5.0 (mm h^{-1})	Accepted by $\lvert q^{6h} - q^{b}\rvert$ QC check
Rain	Rain	1905	1102	1072	944
Rain	No rain	201	58	56	47
No rain	Rain	5781	1182	1182	796
Subtotal		7887	2342	2310	1787

* Total number of $1° \times 1°$ observations: 10 480. Nonraining grids in both observations and the model: 2593.

b. Data usage

The single footprint, instantaneous surface rain retrievals from the TMI and two SSM/I (*F13* and *F14*) sensors using the Goddard Profiling (GPROF) algorithm (Kummerow et al. 1996; Olson et al. 1996) are accumulated over 6 h centered at analysis times and averaged to $1° \times 1°$ GEOS-3 grids. As microwave retrievals over land are less reliable than those over oceans, we restrict the data usage to oceanic areas within 30°N and 30°S, subject to two online QC checks based on the O–B residual in 6-h rain accumulation. First, a gross check is used to eliminate outliers with O–B residuals greater than 5 mm h^{-1}, as the minimization procedure would fail for excessively large O–B values. Data rejected by this criterion typically account for less than 0.5% of all valid observations. Second, if the O–B residual is less than 1 mm in 6 h (i.e., 0.17 mm h^{-1}), no minimization is performed so that data are used only when the background rain is appreciably different from the observed. Since low rain rates account for much of the observed and model precipitation, this minimum threshold has the practical advantage of reducing the computational cost without compromising the quality of the analysis.

With a nonlinear precipitation observation operator, it is possible for the minimization procedure to produce large moisture tendency corrections concentrated at the low levels for a moderate change in surface rain. Instead of using a Jacobian-based preanalysis QC check on moisture (e.g., Treadon et al. 2002), an after-analysis check is applied to the solution to (1) to prevent moisture at the end of the 6-h column model integration, q^{6h}, from deviating from the background values by more

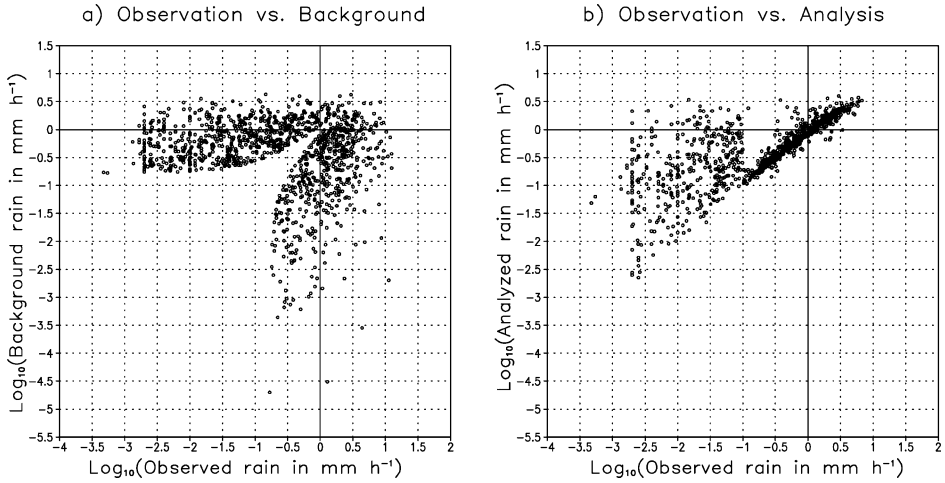

FIG. 3. (a) Background rain vs observations at 1200 UTC 20 Aug 1998. Shown are rain rates at 1072 grid locations accepted by O–B QC checks for minimization. Not included are locations with no rain in either the background or the observation. (b) Analyzed rain rates given by (1) accepted by after-analysis QC checks vs observations. The scatter at very low rain rates reflects the large error standard deviations assigned to observed rain rates below 0.1 mm h^{-1} (see section 2).

than a certain amount. The cutoff value is two standard deviations of the tropical-mean O–F bias in specific humidity in negative O–B cases and three standard deviations in positive O–B cases. These cutoff values are obtained empirically from online assimilation experiments based on root-mean-square (rms) error reductions in daily tropical precipitation (relative to TMI and SSM/I rain rates) and all-sky outgoing longwave radiation (against CERES measurements). The larger threshold value for positive O–B cases reflects that the VCA scheme is more effective in reducing than enhancing the background rain. Typically, 20% of the number of minimizations performed are rejected by this after-analysis check.

The data usage at a single analysis time is illustrated in Table 3 for 1200 UTC 20 August 1998. Of 10 480 valid TMI and SSM/I tropical observations averaged to $1^\circ \times 1^\circ$ model grids, the O–B residual is nonzero at 7887 locations, including 5545 locations at which the model rain is within 0.17 mm h^{-1} of the observed value and no minimization is performed. Of the 2310 minimization solutions, 1787 are accepted by the after-analysis QC check. Altogether, 555 of the 7887 observations (7%) are rejected by the two QC checks. The relatively low data ingestion ratio of 23% reflects that, over 70% of the 7887 data points, the 6-h observation operator produces rain accumulations sufficiently close to observations so as not to invoke minimization. This data usage ratio will likely increase as observations are assimilated with a higher temporal frequency, as done at operational NWP centers (e.g., Marecal and Mahfouf 2000; Treadon et al. 2002). Table 3 also shows that the VCA scheme is effective in assimilating rain rates at locations of zero background rain. However, for the GEOS-3 DAS, the benefits are limited by the fact that the background rain is zero at only 10% of all locations with observed rain.

Figure 3 compares the column-model background rain and analyzed rain from (1) against observations. Figure 3a shows the background rain plotted against observations at 1072 ''raining'' grid locations at which the minimization was performed—excluded are locations of zero rain in either the background or the observation. Figure 3b shows that the 944 analyzed rain rates accepted by the after-analysis QC check lie predominantly along the diagonal against observations, with smaller observation-minus-analysis (O–A) residuals than the corresponding O–B residuals in Fig. 3a. The positive bias in O–A reflects that turning off the model rain is easier than enhancing it since the value of δq is bounded from above by the high relative humidity in the Tropics. These results confirm that the continuous application of moisture time-tendency corrections over 6 h is effective in overcoming systematic errors in the column model to produce analyzed rainfall that better matches observations. One notable exception is the scatter at observed rain rates below 0.1 mm h^{-1}. This is a direct consequence of the larger errors assigned to these low rain rates preventing the solution from overfitting less reliable data (see section 2). The associated sharp transition in Fig. 3b suggests that the minimization solution is indeed responsive to observation error specifications and that the usage of rainfall data could be further improved as better observation error estimates become available.

4. Bonnie and Floyd assimilation experiments

A prominent atmospheric feature difficult to capture accurately in current global models and analyses is the

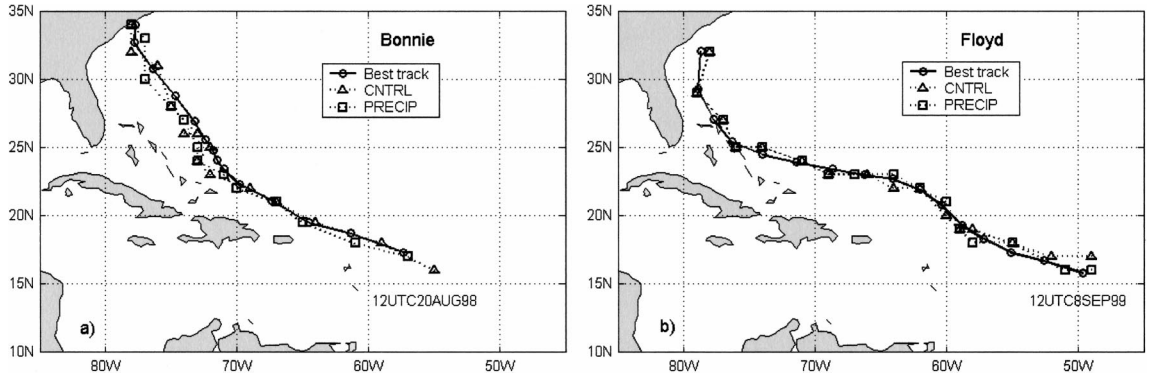

FIG. 4. Analyzed 12-h positions of the minimum surface pressure of (left) Bonnie and (right) Floyd (rendered to the closest integer degree in latitude and longitude) from CNTRL and PRECIP analyses, compared with NOAA best-track locations. The first analysis time of the track is marked for each storm.

tropical cyclone system with fine structures that require a resolution better than one-sixth of a degree to adequately resolve (Kurihara et al. 1990). Yet, an accurate depiction of such systems in analyses is crucial for providing realistic initial conditions for numerical weather forecasts and boundary forcing for nested regional models. Since intense rainfall is associated with hurricane events, precipitation assimilation may be expected to directly affect the representation of hurricanes in global systems. In this study we examine how assimilating tropical TMI and SSM/I surface rain rates over oceans affects $1^\circ \times 1^\circ$ GEOS-3 analyses and forecasts of two distinctly different Atlantic storm systems—Hurricanes Bonnie and Floyd—from the 1998–99 period. As a tropical storm, Bonnie was characterized by a notably asymmetric vortex with a wind maximum to the northeast of the center, while Floyd was much less asymmetric in its early stages of development. For each storm, we performed two parallel assimilation experiments—one (PRECIP) with and one (CNTRL) without TMI and SSM/I rain rates—for a 2-week period centered around the time when the system became a hurricane.

Bonnie reached tropical storm intensity at 1200 UTC 20 August 1998 and subsequently became a hurricane with a nearly complete eyewall by 0000 UTC 22 August (Avila 1998). It eventually made landfall near Wilmington, North Carolina, on 27 August. The period for Bonnie CNTRL and PRECIP assimilation experiments extends from 15 to 29 August. Floyd can be traced to a tropical depression east of the Lesser Antilles on 7 September 1999. The system intensified to a tropical storm at 0600 UTC 8 September and was upgraded to a hurricane by 1200 UTC 10 September near the northern Leeward Islands (Pasch et al. 1999). Floyd made landfall near Cape Fear, North Carolina, on 16 September, then moved on to New England. The Floyd CNTRL and PRECIP assimilation experiments extend from 3 to 17 September.

5. Impact on analyses

Hurricane vortices in global analyses with limited spatial resolution are generally weak, overly smooth, and not as sharply defined compared with observations (Pu and Braun 2001). Rainfall assimilation is not expected to overcome such inherent limitations in model resolution. This section examines the extent to which assimilating TMI and SSM/I surface rain rates may improve the synoptic features of Bonnie and Floyd as realized in the $1^\circ \times 1^\circ$ GEOS-3 analyses.

a. Track trajectory and intensity

Figure 4 compares analyzed positions of the minimum surface pressure of Bonnie and Floyd at 12-h intervals with the ''best track'' published by the Hurricane Research Division (HRD) of National Oceanic and Atmospheric Administration (NOAA). Each track traces the system from the tropical storm stage to the time just before landfall. The GEOS-3 tracks of Bonnie and Floyd, with or without rainfall data, are in general agreement with the best track to within the 1° accuracy of their analyzed positions, which are rendered to the closest integer degree in latitude and longitude. There are instances that rainfall assimilation improves the storm position by more than 1°, as for Bonnie at 1200 UTC 20 August 1998 (the first plotted position) shown in Fig. 4a.

The along-track sea level pressure (SLP) minimum and 850-hPa vorticity are shown in Fig. 5. As noted earlier, hurricanes in global analyses are typically weak. In the early stages when Bonnie and Floyd are tropical storms, the minimum pressures in the CNTRL analyses are within 5 hPa of the best-track values. But as the storms intensified to hurricane strengths, the limited resolution of $1^\circ \times 1^\circ$ analyses cannot capture the rapid surface pressure deepening seen in point observations (Bonnie reached 954 hPa at 0000 UTC 24 August 1998, and Floyd reached 921 hPa at 1200 UTC 13 September

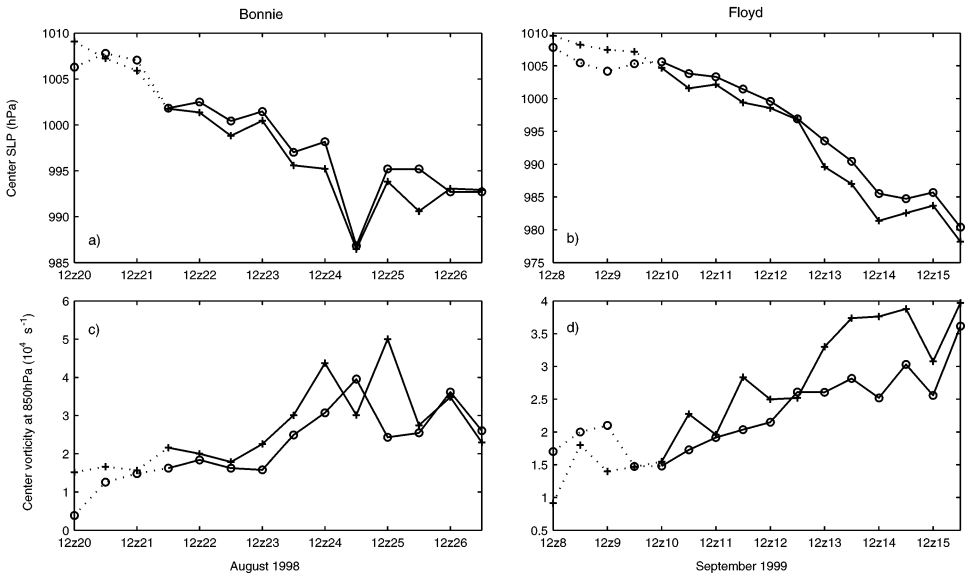

FIG. 5. (a) Minimum SLP in mm day^{-1} along the track of Tropical Storm Bonnie (dotted lines) and Hurricane Bonnie (solid lines). The open circles show the CNTRL analysis and the crosses are the PRECIP analysis. (b) Same as (a), but for Floyd. (c) The 850-hPa vorticity in units of 10^{-4} s^{-1} along the Bonnie track. (d) Same as (c), but for Floyd.

1999). Figure 5 shows that rainfall assimilation yields slightly lower pressure minima and enhanced low-level cyclonic vorticity, suggestive of some positive impact on the storm intensity throughout the hurricane stage. However, rainfall assimilation does not necessarily lead to a lower sea level pressure minimum or stronger low-level vorticity for a variety of reasons. For one, its impact may be to relocate the storm center instead of strengthening a correctly positioned storm, as in the case of Bonnie at 1200 UTC 20 August 1998. Also, assimilation of rain rates from a partial satellite coverage that misses a major section of the storm (as during the early stages of Tropical Storm Floyd) can lead to aliasing problems by modifying the latent heating only in the observed portion of the storm, thereby misrepresenting the circulation pattern. These issues will require further scrutiny beyond the scope of this study.

b. Precipitation and sea level pressure

The impact of assimilating TMI and SSM/I rainfall data on precipitation analyses is manifest in Fig. 6, which shows reduced daily mean rms errors and improved spatial correlations within a 20° latitude × 30° longitude moving domain along the storm tracks. The one exception is the result for Bonnie on 26 August, at which time the storm was entirely north of 30°N, beyond the domain of rainfall assimilation in these experiments.

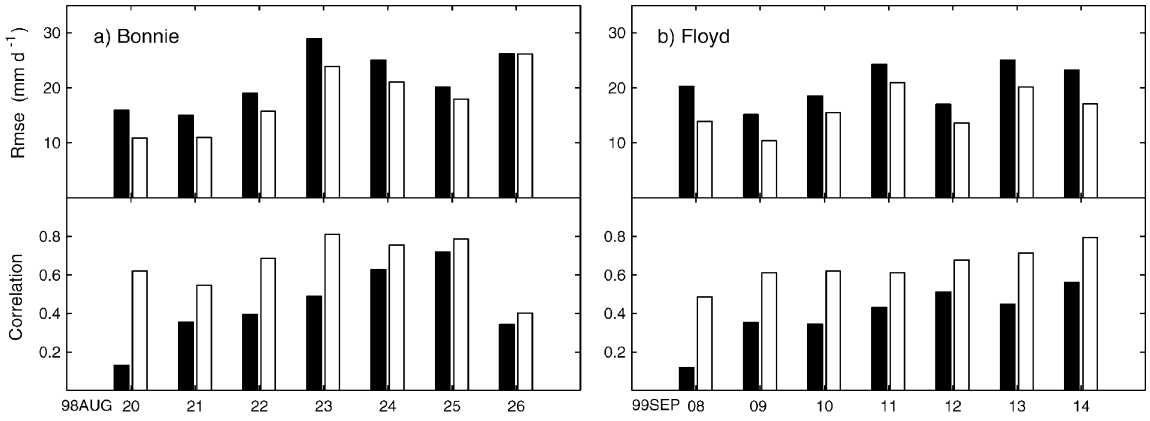

FIG. 6. (a) Rms errors and spatial correlation of daily averaged rain rate over a 20° latitude × 30° longitude moving domain along Bonnie's track. The black and white bars refer to CNTRL and PRECIP analyses, respectively. Combined TMI and SSM/I daily rain rates are used for verification. (b) Same as (a), except for Floyd.

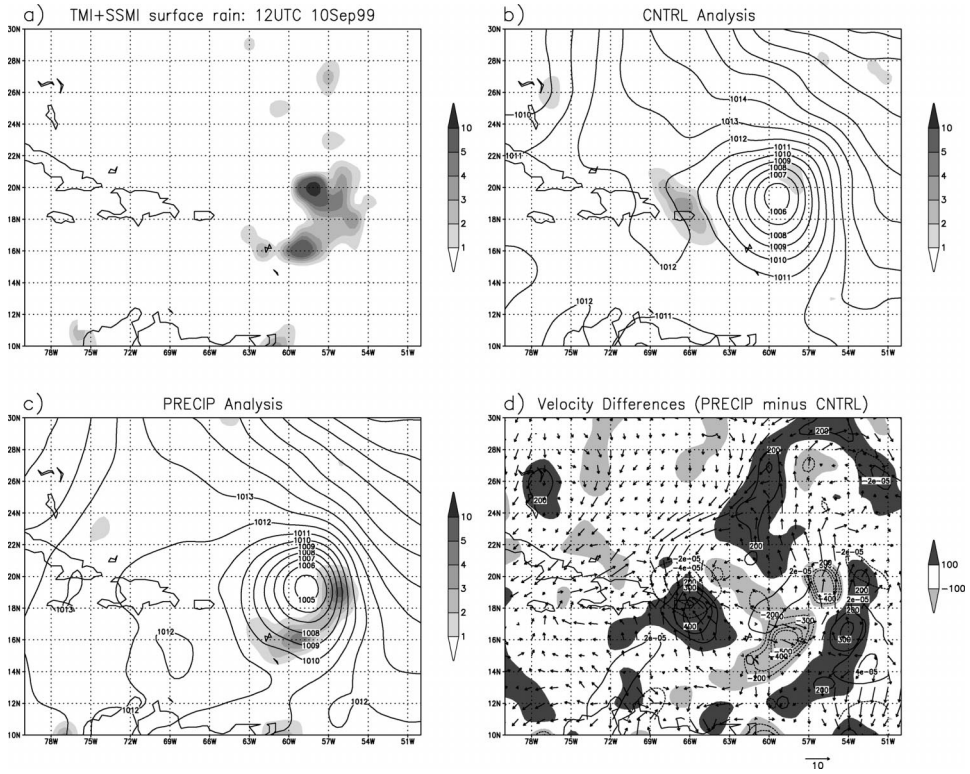

FIG. 7. (a) Combined TMI and SSM/I observations of Floyd surface rain in mm h^{-1} at 1200 UTC 10 Sep 1999. (b) Surface rain in mm h^{-1} (shaded) and SLP in hPa (contours) in CNTRL at the same analysis time. (c) Same as (b), except for PRECIP analysis. (d) Changes between PRECIP and CNTRL analyses in 500-hPa omega velocity in hPa d^{-1} (shaded, with negative values indicating rising motion), divergence in s^{-1} (contour interval of 2×10^{-5} s^{-1} with zero omitted), and horizontal winds in m s^{-1} at 200 hPa. The vector scale for 10 m s^{-1} is given for reference. Note that the heavy observed rainfall maximum in Fig. 7a is flagged by the preanalysis QC check since the background rain is zero at this location (Fig. 7b) and the O–B exceeds 5 mm h^{-1}.

These results show an overall improvement in both the intensity and spatial pattern of precipitation associated with the storm system. For rain rates averaged over the entire Tropics for the 2-week assimilation period, the improvements are even greater. For example, in the case of Bonnie, rainfall assimilation yields a bias reduction of 61% and a smaller error standard deviation by 33%, averaged over the entire Tropics.

Illustrated in Fig. 7 are improved rainfall intensity and structure for Floyd at 1200 UTC 10 September 1999. The storm center in the CNTRL analysis coincides with the best-track position and remains unchanged with the addition of rainfall data. Relative to TMI and SSM/I observations, the rms error of the CNTRL rainfall analysis is 1.03 mm h^{-1} over the domain shown in Fig. 7. Rainfall assimilation reduces the runs error in the PRECIP analysis by 21% and increases the spatial correlation from 0.14 to 0.64. The VCA algorithm is effective in removing the spurious rainfall centered around 19°N and 66°W in the CNTRL (Fig. 7b) and enhancing precipitation in the east and south quadrants of the hurricane vortex (Fig. 7c), consistent with observations. However, the observed heavy rainfall maximum in Fig. 7a was not assimilated since the O–B value exceeded 5 mm h^{-1} relative to the zero background rain shown in Fig. 7b and the data did not pass the preanalysis QC check. Within the IAU analysis framework, precipitation assimilation can directly alter the vertical motion field over 6 h and substantially modify the large-scale circulation. Averaged over the domain shown in Fig. 7d, the spatial correlation between changes in the surface rain field and the 500-hPa omega velocity is −0.71. Note that not all changes in Fig. 7d are the result of rainfall assimilation within the 6-h analysis window since they are the differences between two sequential analyses that started a week earlier on 3 September. But in the immediate neighborhood of the improved 6-h rain accumulation, there is clear evidence of increased horizontal divergence at 200 hPa to the south and east of the storm center and enhanced subsidence at 500 hPa in the surrounding areas away from the hurricane vortex. A more realistic subsidence environment not only promotes a more confined hurricane structure but is also crucial for preventing the low-level moisture from precipitating outside the storm, which is a common problem in global systems (as in the CNTRL). Typically, rainfall

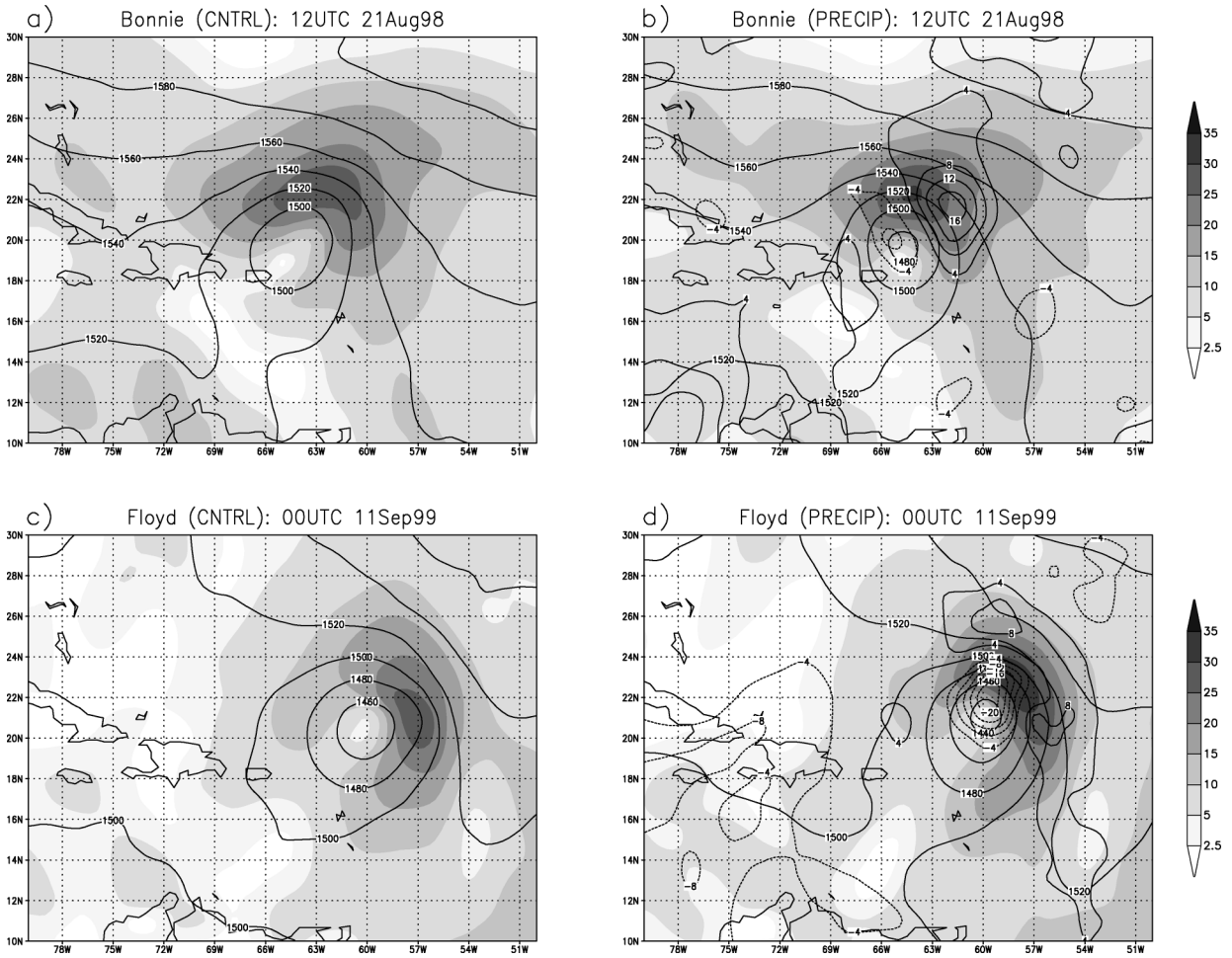

FIG. 8. Analyses of 850-hPa geopotential height in m (thick line) and wind speed in m s^{-1} (shaded). (a) CNTRL analysis at 1200 UTC 21 Aug 1998 for Bonnie. (b) Same as (a), but for PRECIP analysis. The thin contours show PRECIP minus CNTRL differences in 850-hPa geopotential height. (c) CNTRL analysis for Floyd at 00 UTC 11 Sep 1999. (d) Same as (c), but for PRECIP analyses with the thin lines showing 850-hPa geopotential height differences between PRECIP and CNTRL.

assimilation can modify, through continuous δq forcing over 6 h, the horizontal divergent winds at 200 hPa by as much as 10 m s^{-1}, which can have a large impact on short-range forecasts, as will be shown in section 5.

c. Storm structures

Figure 8a shows CNTRL analyses of the 850-hPa geopotential height and wind speed for Bonnie at 1200 UTC 21 August, 12 h before Bonnie gained hurricane strength. The storm center inferred from the minimum wind speed is in agreement—to within 1° of horizontal resolution—with the best-track position of 19.5°N and 64.5°W. The system is, however, too weak with overly broad features compared with observations (Avila 1998). The same quantities from the PRECIP analysis are shown in Fig. 8b, superimposed with the geopotential anomaly between the two analyses, which is negative at the storm center and positive to the east and west, reflecting a deeper and more contracted system with increased horizontal winds to the north of the storm center. This north–south asymmetry is consistent with wind observations from ships and high-resolution low-cloud wind analysis (Avila 1998). Changes in these fields at other levels indicate an overall intensification of the storm in the lower troposphere and a slight weakening above the midtroposphere, leading to a more realistic structure typical of tropical storm systems. These changes are evident in the vertical structure of a meridional cross section through the center of Bonnie shown in Figs. 9a, 9b, and 9c. Compared with the CNTRL, the PRECIP analysis shows a better-defined vortex structure with a distinct eyelike feature (identified by a column of low wind speed), a more pronounced warm core in the midtroposphere, and an enhanced low-level vorticity maximum (by more than 40%), all characteristic of hurricane structures inferred from in situ observations (e.g., Anthes 1982). Again, Fig. 9c shows that the observed north–south asymmetry of Bonnie is also better captured in the PRECIP analysis, with stron-

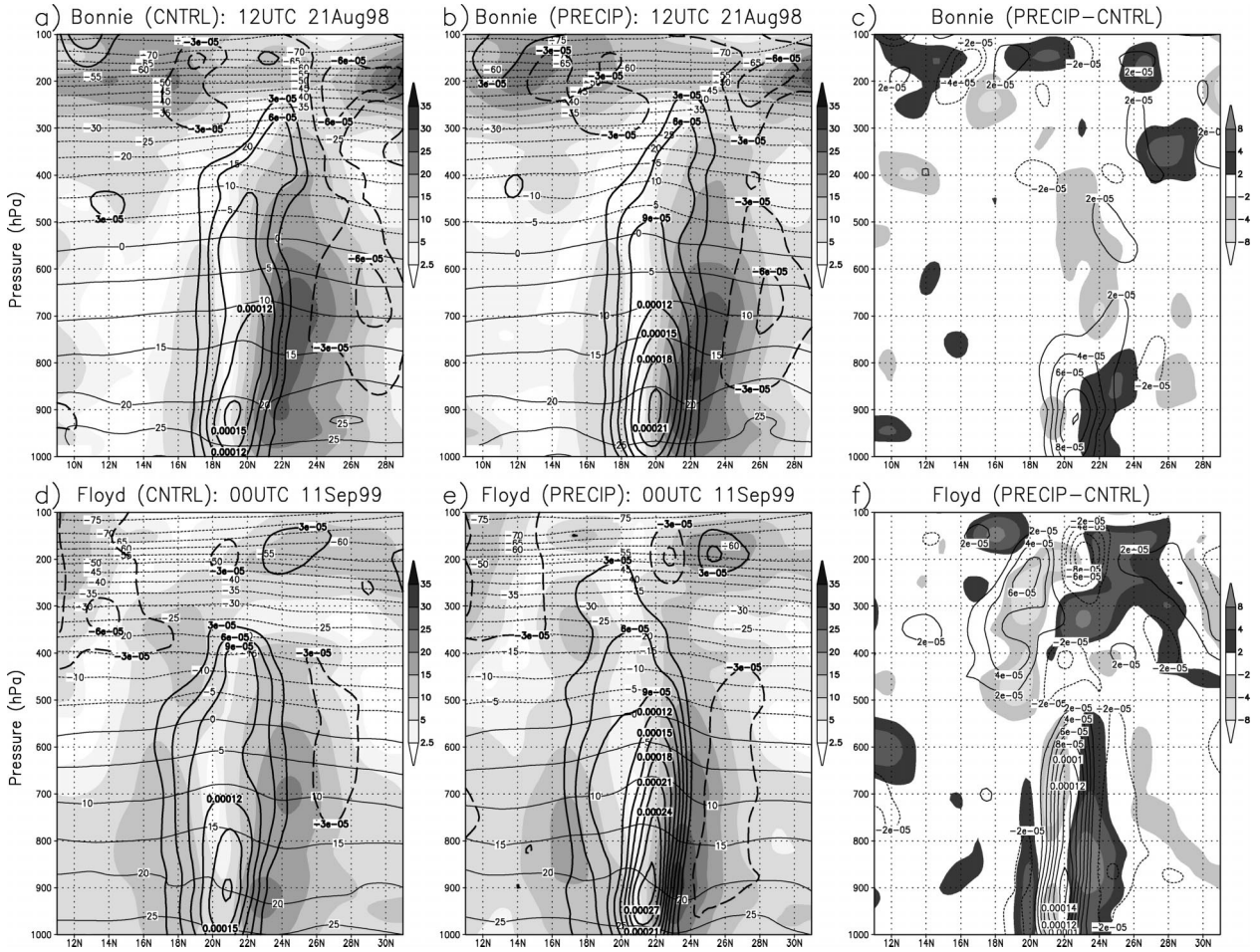

FIG. 9. (a), (b) The meridional–vertical cross sections at 65°W through the center of Bonnie at 1200 UTC 21 Aug 1998 from the CNTRL and PRECIP analyses, respectively. Displayed are wind speed in m s^{-1} (shaded), relative vorticity in s^{-1} (thick lines at intervals of 3×10^{-5}, with the zero contour omitted), and temperature in °C (thin lines). (c) The difference between PRECIP and CNTRL analyses, with wind speed shaded at intervals of ±(2, 4, and 8) m s^{-1} and vorticity contours at intervals of 2×10^{-5} s^{-1}, with the zero contour omitted. (d), (e) Similar cross sections for Floyd at 60°W and 0000 UTC 11 Sep 1999, with the difference shown in (f).

ger low-level winds to the north of the storm center and weaker winds to the south.

Hurricane vortices in global models are generally too weak at the low levels yet too strong at the upper levels, leading to an incorrectly placed wind maximum in the analysis compared with observations. Rainfall assimilation acts to strengthen the low-level winds and weaken winds between 700 and 400 hPa, as shown in Fig. 9c, although it is even more evident in the zonal cross section (not shown). This downward displacement of the wind maximum (and the kinetic energy maximum) is similar to what is often achieved by imposing an artificial ''bogus'' vortex to improve hurricanes in analyses (e.g., Lord 1991). However, the bogusing technique has several well-known limitations: It can be applied only to mature hurricanes; it does not perform well for highly asymmetric storm systems; and specifying a moisture field consistent with the imposed vortex is often problematic (Pu and Braun 2001). Precipitation assimilation using the VCA scheme offers an alternative to bogusing that is more consistent with model physics and applicable in early stages of storm development regardless of the azimuthal asymmetry. However, the benefit of rainfall assimilation is currently limited by model resolutions. As models continue to evolve to finer resolutions, precipitation assimilation has the potential of being an effective method for improving the realism in storm analyses and early-warning capabilities.

In the case of Floyd, similar improvements are even more evident. Figure 8c and 8d show the 850-hPa geopotential height and wind speed at 0000 UTC 11 September 1999, shortly after Floyd reached hurricane strength. The PRECIP analysis shows a substantially stronger storm, with a clearly defined center coinciding with the best-track position at 20.8°N and 60.4°W. The 850-hPa height anomaly is negative to the north of the storm center in the CNTRL, signifying a deepening and a northward shift, with an overall increase in intensity

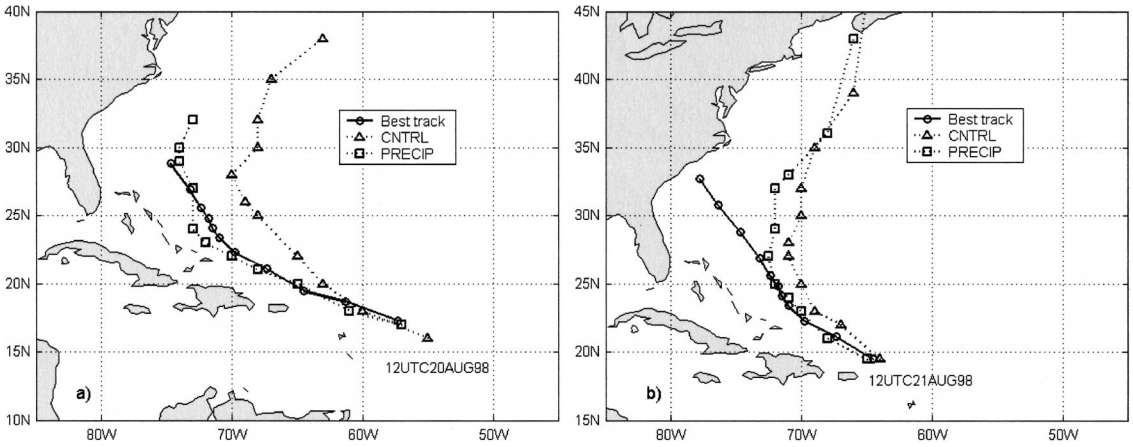

FIG. 10. Five-day Bonnie track forecasts. Triangles and squares mark forecasts (dashes) initialized with CNTRL and PRECIP analyses, respectively. The storm positions rendered to the closest integer degree in latitude and longitude are plotted every 12 h. The circles show positions of the best track (solid). (a) Forecasts issued from 1200 UTC 20 Aug 1998. (b) Forecasts issued from 1200 UTC 21 Aug 1998.

and compactness of the hurricane at the low levels. Figures 9d, 9e , and 9f show a clear downward displacement and intensification of the low-level wind maximum. The double maxima at 900 and 700 hPa to the north of the center in the CNTRL analysis disappears, leaving only one enhanced maximum near 900 hPa in the PRECIP analysis. Figures 9d and 9e also show that the PRECIP case has a more pronounced warm core and a better-defined eyelike feature in the column of low-speed winds. Analysis of horizontal winds between 200 and 300 hPa shows that the upper-level wind anomaly in Fig. 9f corresponds to a northward shift of a southwesterly jet (to the northwest of the storm center) by a stronger anticyclonic outflow from Floyd in the PRECIP analysis. This increased upper-level outflow is manifest in the anticyclonic vorticity anomaly at 200 hPa in Fig. 9f, which also shows a secondary anticyclonic vorticity anomaly at 400 hPa reflecting a downward shift of the low-level cyclonic vorticity, whose strength effectively doubles between 1000 and 500 hPa above the storm center, as evident in Figs. 9d and 9e. The impact of these improved structures on the forecast is examined in the next section.

6. Impact on forecasts

Results in the previous section showed that rainfall assimilation can significantly modify moisture, wind, and temperature analyses. To assess the impact of these changes on the forecasts, we perfomed parallel Bonnie and Floyd forecasts initialized with PRECIP and CNTRL analyses, with and without rainfall data, respectively. The initial conditions are from the early stages of hurricane formation starting with the first analysis level with a well-formed inner core, namely, 1200 UTC 20 August 1998 for Bonnie, which had just gained tropical storm intensity (Avila 1998) and 1200 UTC 10 September 1999 for Floyd, which had just become a hurricane (Pasch et al. 1999). Four forecasts were issued 12 h apart for each storm over the subsequent 2-day period.

Comparisons of storm track forecasts with the NOAA best-track analysis are shown in Fig. 10 for Bonnie and Fig. 11 for Floyd. The impact ranges from positive to near neutral. Hurricanes in forecasts initialized with CNTRL analyses consistently move too fast along paths that are displaced eastward and northward relative to the best track. In the best cases (Figs. 10a and 11b), forecasts initialized with PRECIP analyses show significant reductions in both spatial and temporal displacement errors. These tend to be associated with initial conditions with significant improvements in both the storm intensity and position. In other cases, forecast improvements reflect mostly reduced errors in spatial locations rather than temporal displacements, as in Figs. 10b and 11a. Other forecasts issued during the 2-day periods show similar improvements that fall within the ranges shown in Figs. 10 and 11.

To verify that the improvements shown in Figs. 10 and 11 result directly from assimilating rainfall information in the initial conditions, we varied the assigned weighting for the TMI and SSM/I rain rates in the VCA procedure to investigate how the resulting analyses affect storm forecasts. In addition to CNTRL and PRECIP analyses (for which the precipitation observation error standard deviation, σ_o, is effectively infinity and 30%, respectively), we obtained two more PRECIP analyses with σ_o = 80% and 250% and performed additional forecasts using them as initial conditions. Results for the 5-day Bonnie forecast issued from 1200 UTC 20 August 1998 are shown in Fig. 12. As the initial analysis is weighted more toward the TMI and SSM/I rain rates, there is a systematic improvement in the track forecast (Fig. 12a) and an overall increase in the spatial correlation between the 5-day precipitation forecast and observations (Fig. 12b). The exception is the rain forecast

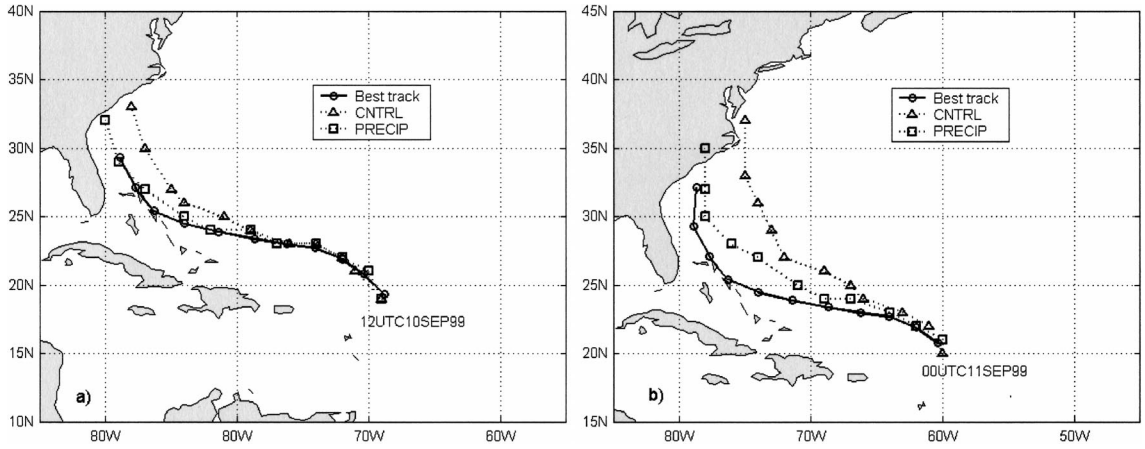

FIG. 11. Five-day Floyd track forecasts. Triangles and squares mark forecasts (dashes) initialized with CNTRL and PRECIP analyses, respectively. The storm positions rendered to the closest integer degree in latitude and longitude are plotted every 12 h. The circles show positions of the best track (solid). (a) Forecasts initialized from 1200 UTC 10 Sep 1999. (b) Forecasts issued from 0000 UTC 11 Sep 1999.

within the first 24 h, in which case the forecast differences are likely too small to overcome measurement and sampling uncertainties in rainfall observations. The overall results indicate a systematic increase in forecast skills as more rainfall information is retained in the initial state, suggesting that the improvements are directly attributable to the use of rainfall data in the initial condition.

Shown in Fig. 13 are two examples of the rms errors and spatial correlations in 5-day precipitation forecasts issued from analyses with and without TMI and SSM/I rain rates. The Bonnie forecast (Figs. 13a and 13c) was issued from 1200 UTC 20 August 1998. The Floyd forecast (Fig. 13b and 13d) was initialized from 0000 UTC 11 September 1999. In each case, the statistics are for a 20° latitude by 30° longitude moving domain along the analyzed storm track. Results show a general reduction in rms errors and a marked increase in spatial correlations. These improvements are also apparent in terms of the improved threat scores for different rain thresholds commonly used to assess quantitative precipitation forecast (QPFs; Wilks 1995) skills.

7. Summary and discussion

We have described a VCA algorithm for assimilating surface precipitation using a 1D forecast model as a weak constraint and examined its effectiveness in using 6-h TMI and SSM/I tropical rain rates to improve GEOS-3 analysis and forecasts. This 1D variational continuous rainfall assimilation scheme, in its full implementation, uses temperature and moisture time-tendency corrections to compensate for model deficiencies. But the current understanding of the error characteristics of

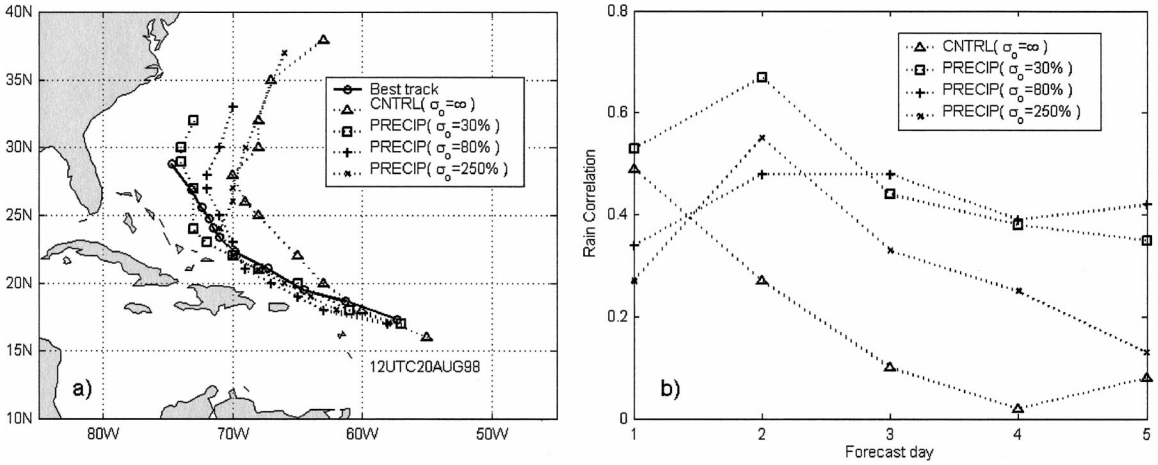

FIG. 12. Sensitivity of a 5-day Bonnie forecast from 1200 UTC 20 Aug 1998 to TMI and SSM/I rainfall information retained in the initial condition. (a) Comparison of 5-day track forecast with the NOAA best-track analysis. (b) Spatial correlations between 5-day precipitation forecasts and combined TMI and SSM/I daily rain rates. The legend identifies the forecasts by the error standard deviation for rain (σ_o) in the analysis used for initial condition.

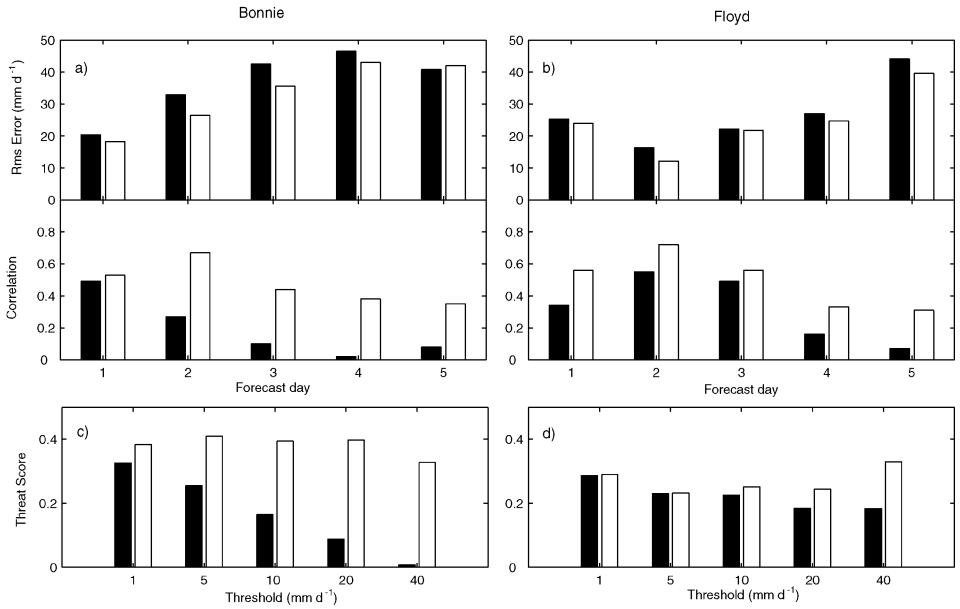

FIG. 13. Rms errors and spatial correlations of 5-day precipitation forecasts initialized with CNTRL analysis (black) and PRECIP analysis (white). (a) Bonnie forecast issued from 1200 UTC 20 Aug 1998. (b) Floyd forecast issued from 0000 UTC 11 Sep 1999. The statistics are for a 20° latitude by 30° longitude moving domain along the analyzed storm track. (c), (d) QPF threat scores for the day 3 precipitation forecast for Bonnie and Floyd, respectively. A higher threat score indicates greater forecast skills.

the 1D moist process model is very limited, making it premature to attempt a data impact assessment using the full scheme with both temperature and moisture tendency corrections. Since the model-predicted rain is diagnostically linked to the time rate of change of the atmospheric moisture, corrections on the moisture time tendency alone can be an effective control variable for assimilating rainfall data. This is the focus of this study.

In earlier studies we have shown that assimilating TMI and SSM/I rain rates improves the precipitation analysis and related climate parameters such as radiative fluxes and cloud forcing in the GEOS analysis. The present research focused on the impact of rainfall assimilation on $1° \times 1°$ GEOS-3 analyses and forecasts of synoptic features of prominent tropical weather systems using Hurricanes Bonnie and Floyd as case studies. For each storm, we performed two parallel assimilation experiments with and without rainfall data. Results show that assimilating TMI and SSM/I surface rain using the 1DVCA scheme with moisture time-tendency corrections yields more realistic analyzed storm structures. Forecast experiments show that the improved analyses also provide better initial conditions for 5-day track and QPF scores for Bonnie and Floyd. The improved forecast skills have been substantiated in a sensitivity study that showed a systematic increase in forecast skills as more rainfall information was retained in the initial condition.

Results of this study show that addressing model deficiencies is an important consideration in precipitation assimilation. They also suggest that the full benefit of precipitation assimilation can be realized only if analyses of wind, temperature, moisture, and pressure are allowed to respond to an improved rainfall analysis within an assimilation cycle. Understandably, as a model-diagnosed quantity, precipitation affects forecasts only through its influence on the model's prognostic variables. In the GEOS-3 DAS, the prognostic variables continually adjust to changes in precipitation and the associated latent heating field over a 6-h assimilation window, in a manner similar to dynamic initialization. Results show that assimilating rainfall data through time-continuous corrections of moisture tendencies is effective for improving the instantaneous state variables used to initialize the forecasts.

As a technique for rainfall assimilation, the 1DVCA scheme differs from nudging or physical initialization in that it is a statistical analysis within the optimal estimation framework, even though they all modify the model's prognostic tendencies. As implemented in the GEOS-3 DAS, the VCA scheme effectively operates as an online model bias estimation and correction for precipitation and moisture every 6 h. Given its nonstatic nature, the VCA scheme is suitable for assimilating time-accumulated precipitation and is thus less restricted by the problem of ''zero background rain'' as compared to static 1DVAR/3DVAR of instantaneous rain rates. More generally, VCA time-tendency corrections may be included as a part of an augmented control variable within the 4DVAR framework or as a model error estimator in sequential analysis schemes.

Last, we note that in our work thus far, the 1DVCA

scheme has been shown to be effective for assimilating rainfall data in the Tropics, where the model precipitation is known to be sensitive to parameterized moist physics in a vertical column. The effectiveness of 1D VCA approach to rainfall assimilation in the extratropics, where atmospheric processes are governed by multivariate quasigeostrophic dynamics, will require further investigation.

Acknowledgments. It is a pleasure to acknowledge the support of this work through the TRMM Science Team under NASA Headquarters TRMM Program Scientist, Dr. Ramesh Kakar. We would also like to thank an anonymous reviewer for a thoughtful review of the manuscript and constructive comments that led to substantive improvements of this paper.

REFERENCES

Anthes, R., 1982: *Tropical Cyclones: Their Evolution, Structure and Effects. Meteor. Monogr.,* No. 41, Amer. Meteor. Soc., 208 pp.

Avila, L., 1998: Preliminary report: Hurricane Bonnie: 19–30 August 1998. National Hurricane Center, Miami, FL, 10 pp. [Available online from http://www.nhc.noaa.gov/1998bonnie.html.]

Bauer, P., J.-F. Mahfouf, W. S. Olson, F. S. Marzano, S. di Michele, A. Tassa, and A. Mugnai, 2002: Error analysis of TMI rainfall estimates over ocean for variational data assimilation. *Quart. J. Roy. Meteor. Soc.,* **128,** 2129–2144.

Bell, T. L., A. Abdullah, R. Martin, and G. North, 1990: Sampling errors for satellite-derived tropical rainfall: Monte Carlo study using a space–time stochastic model. *J. Geophys. Res.,* **95,** 2195–2205.

Bloom, S. C., L. L. Takacs, A. M. da Silva, and D. V. Ledvina, 1996: Data assimilation using incremental analysis updates. *Mon. Wea. Rev.,* **124,** 1256–1271.

Cohn, S., 1997: An introduction to estimation theory. *J. Meteor. Soc. Japan,* **75,** 257–288.

——, A. da Silva, J. Guo, M. Sienkiewicz, and D. Limbic, 1998: Assessing the effect of data selection with the DAO Physical-space Statistical Analysis System. *Mon. Wea. Rev.,* **126,** 2913–2926.

Dee, D. P., and R. Todling, 2000: Data assimilation in the presence of forecast bias: The GEOS moisture analysis. *Mon. Wea. Rev.,* **128,** 3268–3282.

——, and A. M. da Silva, 2003: The choice of variable for atmospheric moisture analysis. *Mon. Wea. Rev.,* **131,** 151–171.

Derber, J. C., 1989: A variational continuous assimilation technique. *Mon. Wea. Rev.,* **117,** 2437–2446.

Fillion, L., and R. Errico, 1997: Variational assimilation of precipitation data using moist convective parameterization schemes: A 1D-var study. *Mon. Wea. Rev.,* **125,** 2917–2942.

——, and J.-F. Mahfouf, 2000: Coupling of moist-convective and stratiform precipitation processes for variational data assimilation. *Mon. Wea. Rev.,* **128,** 109–124.

Hou, A. Y., D. Ledvina, A. da Silva, S. Zhang, J. Joiner, R. Atlas, G. Huffman, and C. Kummerow, 2000a: Assimilation of SSM/I-derived surface rainfall and total precipitable water for improving the GEOS analysis for climate studies. *Mon. Wea. Rev.,* **128,** 509–537.

——, S. Zhang, A. da Silva, and W. Olson, 2000b: Improving assimilated global datasets using TMI rainfall and columnar moisture observations. *J. Climate,* **13,** 4180–4195.

——, ——, ——, ——, C. Kummerow, and J. Simpson, 2001: Improving global analysis and short-range forecast using rainfall and moisture observations derived from TRMM and SSM/I passive microwave sensors. *Bull. Amer. Meteor. Soc.,* **81,** 659–679.

Kessler, E., 1969: *On the Distribution and Continuity of Water Substance in the Atmospheric Circulation. Meteor. Monogr.,* No. 32, Amer. Meteor. Soc., 82 pp.

Krishnamurti, T. N., H. S. Bedi, and K. Ingles, 1993: Physical initialization using SSM/I rain rates. *Tellus,* **45A,** 247–269.

Kummerow, C., W. Olson, and L. Giglio, 1996: A simplified scheme for obtaining precipitation and vertical hydrometeor profiles from passive microwave sensors. *IEEE Trans. Geosci. Remote Sens.,* **34,** 1213–1232.

Kurihara, Y., M. A. Bender, R. E. Tuleya, and R. Ross, 1990: Prediction experiments of Hurricane Gloria (1985) using a multiply nested movable mesh model. *Mon. Wea. Rev.,* **118,** 2185–2198.

Lord, S. J., 1991: A bogusing system for vortex circulations in the National Meteorological Center global forecast model. Preprints, *19th Conf. on Hurricanes and Tropical Meteorology,* Miami, FL, Amer. Meteor. Soc., 328–330.

Marecal, V., and J.-F. Mahfouf, 2002: Four-dimensional assimilation of total column water vapor in rainy areas. *Mon. Wea. Rev.,* **130,** 43–58.

Moorthi, S., and M. Suarez, 1992: Relaxed Arakawa–Schubert: A parameterization of moist convection for general circulation models. *Mon. Wea. Rev.,* **120,** 978–1002.

Olson, W. S., C. D. Kummerow, G. M. Heymsfield, and L. Giglio, 1996: A method for combined passive–active microwave retrievals of cloud and precipitation profiles. *J. Appl. Meteor.,* **35,** 1763–1789.

Pasch, R. J., T. Kimberlain, and S. Stewart, 1999: Preliminary report: Hurricane Floyd: 7–17 September 1999. National Hurricane Center, Miami, FL, 22 pp. [Available online at http://www.nhc.noaa.gov/1999floyd.html.]

Pu, Z. H., and S. Braun, 2001: Evaluation of bogus vortex techniques with four-dimensional variational data assimilation. *Mon. Wea. Rev.,* **129,** 2023–2039.

Randall, D., and Coauthors, 2003: Confronting models with data: The GEWEX Cloud Systems Study. *Bull. Amer. Meteor. Soc.,* **84,** 455–469.

Schubert, S., J. Pfaendtner, and R. Rood, 1993: An assimilated data set for earth science applications. *Bull. Amer. Meteor. Soc.,* **74,** 2331–2342.

Treadon, R. E., H.-L. Pan, W.-S. Wu, Y. Lin, W. Olson, and R. Kuligowski, 2002: Global and regional moisture analyses at NCEP. *Proc. ECMWF/GEWEX Workshop on Humidity Analysis,* Reading, United Kingdom, ECMWF, 33–47. [Available from European Centre for Medium Range Weather Forecasts, Shinfield Park, Reading RG2 9AX, United Kingdom.]

Trenberth, K. E., and J. G. Olson, 1988: An evaluation and intercomparison of global analyses from the National Meteorological Center and the European Centre for Medium Range Weather Forecasts. *Bull. Amer. Meteor. Soc.,* **69,** 1047–1057.

Tsuyuki, T., 1997: Variational data assimilation in the Tropics using precipitation data. Part III: Assimilation of SSM/I precipitation rates. *Mon. Wea. Rev.,* **125,** 1447–1464.

Wilks, D. S., 1995: *Statistical Methods in the Atmospheric Science.* Academic Press, 467 pp.

Zupanski, M., D. Zupanski, D. Parrish, E. Rogers, and G. DiMego, 2002: Four-dimensional variational data assimilation for the blizzard of 2000. *Mon. Wea. Rev.,* **130,** 1967–1988.